TÉCNICO LISBOA

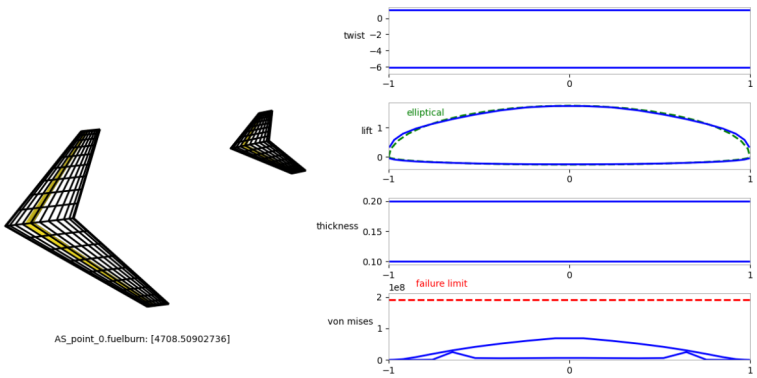

Aircraft Optimal Design

Aerospace Engineering

Luís Martins Pacheco

Number 96425

João Pedro Gaspar

Number 96930

Report #Final Project

02/07/2023

Contents

1 Introduction

The present work aims to present the process of an aerostructural optimization of the wing and horizontal stabiliser of the Bombardier CRJ700 regional commercial aircraft. The aerostructural optimization goal is to decrease the amount of fuel burned during cruise flight. The baseline characteristics of this aircraft will serve as the basis for optimizing the wings.

The optimization is performed using OpenAeroStruct, a framework created based on the openMDAO Python API. This software tool enables the optimization of both the aerodynamic part, using a low-fidelity aerodynamic model based on the Vortex-Lattice Method (VLM), and the structural part, through the application of a low-fidelity structural model to the wingbox structure using a formulation with 6 degrees of freedom 3-D spatial beams.

In the analysis two flight conditions will be considered: one where the aircraft is in cruise flight and another where the aircraft is performing a manuever with a load factor of 2.5.

2 Formulation of the optimization problem

In this optimization problem the main and tail wing will be aerostructurally optimized, through multiple design variables, in order to decrease the aircraft cruise fuel consumption for the same distance traveled. The fuselage, vertical stabilizer, and engines will not be modified.

2.1 Baseline

To perform the optimization some baseline values for Bombardier CRJ700 are required, as well as some information about its cruise flight. Table 1 presents some of those values, which were provided in the assignment, and which will serve as the foundation for the optimization.

Specification	**Value**
Range	$R = 1,685 n.mi$
Cruise Mach number	$M = 0.78$
Cruise altitude	$h = 35,000 ft$
Wing span	$b = 23.24 m$
Wing sweep (@c/4)	$\Lambda = 30°$
Wing taper ratio	$\lambda = 0.3$
Wing aspect ratio	$AR = 8$
Thickness/chord ratio (@root)	$t/c = 0.12$
Max. section lift coeff.	$Cl_{max} = 0.6$
Engine SFC (GE CF34)	$SFC = 0.38$
Take-off weight	$TOW = 323,608 N$
Operating empty weight	$OEW = 193,498 N$

Table 1: Baseline data for the Bombardier CRJ700 provided in the assignment.

Besides this values, additional aircraft baseline parameters and other data was required for the opti-

mization.

The initial baseline values for the dimensions and characteristics of the wing and horizontal stabilizer, their location in relation to each other, and the locations of the engines, were determined using Figure 1 [1]. This Figure is a scaled image of the Bombardier CRJ700. All measurements in this figure were taken using *SolidWorks* and afterwards a scale conversion was performed in order to provide estimates for the real life values of the measurements. The conversion factor was determined using:

$$CF = \frac{b_{real}}{b_{measured}} = \frac{23.24}{506.23} = 0.04591 \tag{1}$$

as the real wing span, b_{real}, and the scaled wing span, $b_{mesuered}$, are both known .

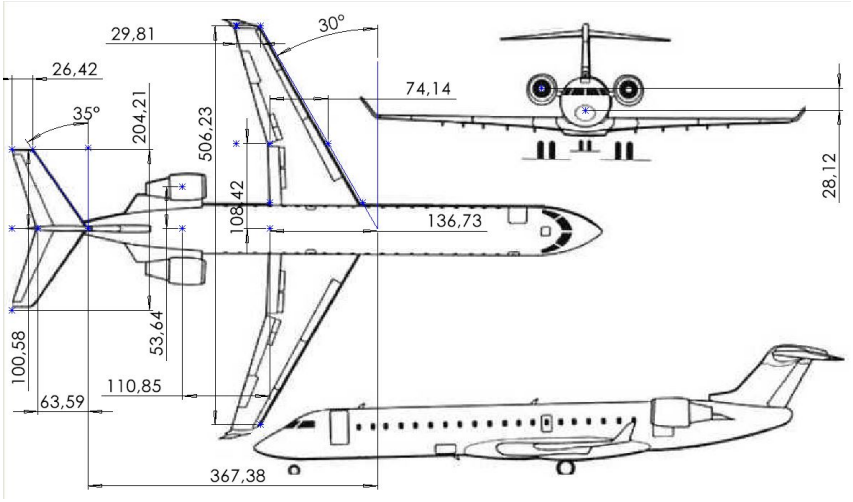

Figure 1: Plane measurements at a scale [1]

The real world measurements, namely the tip and root chords for the wing and horizontal stabilizer, the offset between these lifting surfaces, and the location of the engines are summed up in Table 2.

Parameter	***SolidWorks* Value**	**Real Value**
Main wing span	506.23 mm	23.24 m
Main wing root chord	136.73 mm	6.28 m
Main wing tip chord	29.81 mm	1.37 m
Main wing kink chord	74.14 mm	3.40 m
Main wing kink to root distance	108.42 mm	4.98 m
main wing sweep at root °	30 °	30 °
Tail wing span	204.21 mm	9.37 m
Tail main wing root chord	63.59 mm	2.92 m
Tail main wing tip chord	26.42 mm	1.21 m
Tail wing sweep at root	35 °	35 °
Offset from wing to tail	367.38 mm	16.87 m

Table 2: Conversion of the aircraft scaled measurements to real life estimates

The airfoil profile used for the main wing is the NASA SC2-0612, which is a supercritical profile that has a thickness-to-chord ratio of 12% [2]. As the wingbox model will be used, it is considered that only

10% to 60% of the chord will be structural. The value of CL_0, the lift coefficient of the surface at $\alpha = 0$, was set to 0 and CD_O was set to 0.0078 to account for the drag from the fuselage, nacelles, and pylons (which are not being modeled). The fraction of chord with laminar flow is k_{lam}=0.05 and the chordwise location of maximum thickness is c_{maxt}=0.38.

The wingbox spar and skin thickness distributions and the wing twist distribution have the following control points: $spar_{thickness}$=$[0.004, 0.005, 0.008]$ m, $skin_{thickness}$=$[0.005, 0.01, 0.015]$ m, $twist$=[4,6,8] °. The same thickness for both the top and bottom wing skins are used. Similarly, the same thickness variables for the front and rear spars are also used.

The airfoil profile used for the tail wing is the NACA 0015 which has a thickness-to-chord ratio of 15% [3].The value of CL_0 was set to 0 , CD_O set to 0.015, k_{lam} to 0.05 and c_{maxt} to 0.303. The wingbox spar and skin thickness distributions and the horizontal stabilizer twist distribution have the following control points $spar_{thickness}$ = $[0.002]$ m, $skin_{thickness}$ = $[0.001]$ m, $twist = [3]$ °.

It was defined that for the optimization the viscous effects and the wave drag were to be considered.

The spars and the skin of both the wing and horizontal stabilizer were made of an aluminium alloy, Al 7075-T6. This material has a density of 2810 kg/m^3, a Young's modulus, E, of 71.7 GPa, a shear modulus, G, of 26.9 GPa and a tensile yield stress of 503.31 MPa [4].

The aircraft has two GE CF34 engines located 13 meters behind the leading edge of the wing and 2.45 meters to the side of the longitudinal axis of the airplane. Each engine weights 1200 Kg [5]. For the cruise altitude it was estimated that the fuel density is around 825 kg/m^3 and the wing carries 1000 kg of reserve fuel mass [6].

It was specified that the loads from the weight of the wingbox structure and the weight of the fuel should be distributed on the wing structure to provide load relief. To reduce computational cost during optimization a single constraint was utilized by using the Kreisselmeier–Steinhauser function. Also the $wing_{weightratio}$ was set to 2 to estimate the weight of other components not modeled in the wingbox structure.

Knowing that the airplane cruise altitude is 35 000 ft it was determined that the air density was 0.3796 kg/m^3, that the speed of sound was 296.5 m/s and the dynamic viscosity was equal to 1.422 $\times 10^{-5}$ kg/(m·s). Being the cruise Mach number equal to 0.78, the aircraft cruise velocity is 231.27 m/s. With all this information, and considering the mean chord as the characteristic length, the Reynolds number was calculated to be 23.6 $\times 10^6$.

2.2 Design Variables, Constrains and Objective Function

The goal of the optimization is to minimize fuel consumption for a regional flight of the Bombardier CRJ700. In this aircraft flight profile, two optimization points, cruise and maneuvering, will be considered. Both wing and horizontal stabilizer will be optimized to operate efficiently during these two flight stages.

To begin the optimization process, it is necessary to define the objective function, which, in our case, will be the fuel consumption. The Breguet equation allows the calculation of the fuel consumption based on certain coefficients and the desired range to be achieved.

$$R = \frac{V}{SFC}\frac{C_L}{C_D}\ln\left(\frac{W_{\text{initial}}}{W_{\text{final}}}\right) \tag{2}$$

The parameters in this equation which will be constant in the optimization are: the range R, the flight speed V, and the specific fuel consumption, SFC. All other variables will be adjusted to minimize the fuel mass. Within the initial weight of the aircraft the weight of the fuselage, engines, wings, vertical and horizontal stabilizer and total fuel are considered. The final weight will consider all the same weight parameters except the fuel burned during flight.

To minimize the fuel burned, the aerodynamic coefficient $\frac{C_L}{C_D}$ will need to be maximized and the wing's structural weight minimized.

To maximize the aerodynamic coefficient, the coefficient of drag, C_D, will need to be minimized while the lift coefficient C_L maximized. To minimize the total weight of the aircraft, and therefore the fuel burned during flight, the weight of both the main wing and the tail wing should be reduced, considering that the rest of the aircraft structure remains the same. To minimize the weight of the aircraft, the thickness of the spar and the skin thickness of the two wings are defined as design variables in the problem.

It should be noted that there exists a aerostructural coupling: when maximizing the wing's $\frac{C_L}{C_D}$ and reducing the wings structural weight attention should be paid to the fact that the new lightweight wing structure should be able to support all the loads, including the aerodynamic ones.

The main design variables which will be considered in the optimization to influence the aerodynamic parameters are the cruise and maneuver angles of attack, one for each flight stage, the wing and tail twist, the wing sweep and thickness to chord ratio and the tail span.

The main design variables which will be considered in the optimization to influence the structural parameters are the wing and tail skin and spar thickness as well as the tail span.

During the optimization some constrains should be considered in order to provide results that would make physical sense for an aircraft. For instance during flight the lift coefficient of the aircraft must be equal to the weight, i.e., $L = W$, to ensure level flight. The aircraft should also be trimmed, i.e., $C_M = 0$, meaning its pitching momentum should be zero for both flight stages. To ensure that the aircraft does not stall, it is essential to impose a constraint on the wing profile lift coefficient. The profile lift coefficient cannot reach the critical value, thus $C_l \leq C_{l_{max}}$. As said previously, the lifting surfaces structure should be able to endure the loads imposed on them and therefore a structural failure constrain was added to each surface. A constrain that ensured that all fuel fitted inside the wingbox structure was also required.

The optimization problem can therefore be formulated in the standard form as:

$$
\begin{aligned}
\text{Minimize} \quad & m_{fuelbrun} \\
\text{w.r.t.} \quad & m_{fuel}, \\
& \alpha, \alpha_{manouver}, \\
& \gamma_{wing}, \Delta_{wing}, \delta_{wing_{spar}}, \delta_{wing_{skin}}, t/c \\
& \gamma_{tailwing}, \delta_{tailwing_{spar}}, \delta_{tailwing_{skin}}, b_{tailwing}
\end{aligned}
\tag{3}
$$

$$
\begin{aligned}
\text{subject to} \quad & L = W, \\
& C_M = 0, \\
& C_l \leq C_{l_{max}}, \\
& wing_{failure} = 0, \\
& tailwing_{failure} = 0, \\
& fuel\_vol\_delta \geq 0.
\end{aligned}
\tag{4}
$$

where γ ist the wing twist, Δ is the sweep angle, δ is the thickness, t/c is the thickness to chord ratio and b is the span.

2.3 Mesh size study

After establishing the baseline parameters of the aircraft and in order to proceed to the aerostructural optimization it is crucial to establish an appropriate mesh size to ensure not only efficient computational performance but also that the optimization results are independent of the mesh used.

To do so, a study of the aircraft in cruise was performed in analysis mode. It was defined that the mesh size would vary as follows, where *ny* is the number of elements in the spanwise direction and *nx* the number of elements in the chordwise direction:

- If ny is less than or equal to 11, a fine resolution of 3 is assigned to nx.
- If ny is greater than 11 but less than or equal to 19, a moderately fine resolution of 5 is assigned to nx.
- If ny is greater than 19 but less than or equal to 27, a coarser resolution of 7 is assigned to nx.
- If ny is greater than 27 but less than or equal to 35, a relatively coarse resolution of 9 is assigned to nx.

This progressive adjustment of the mesh resolution, based on the varying values of *ny* facilitates the accurate representation of features and phenomena in the computational domain while optimizing computational resources. In the spanwise direction a cosine spacing of 0.5 was used in order to better

capture the aerodynamic vortices and wing structure deformations which are more pronounced at the wing tip.

From this study Figures 2, 3, and 4 were obtained. Figure 2 represents the variation of the wing and tail lift and drag coefficients with the number of elements in the span wise direction. Figures 3, and 4 represent the variation of the wing tip vertical displacement and fuel burn with the number of elements in the spanwise direction, as well as the CPU time required, respectively. Figure 2 allows us to understand the influence of the number of elements in the aerodynamic parameters, Figure 3 in the structural parameters and 4 in the objective function.

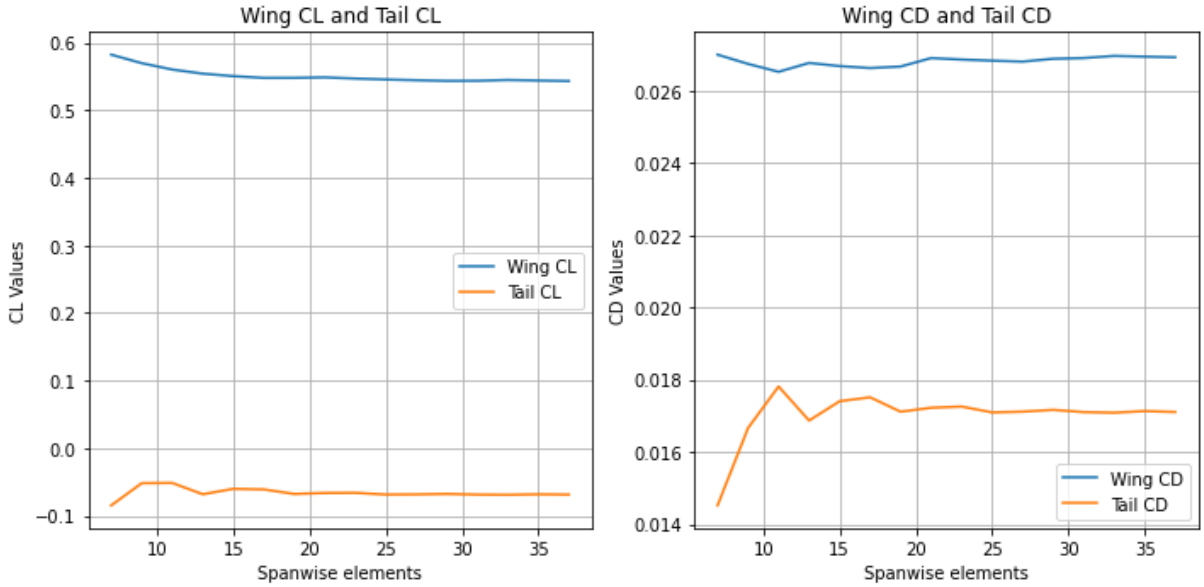

Figure 2: Variation of the Coefficient of Lift the Coefficient of Drag for the wing and tail with the number of spanwise elements of the mesh, left-hand side and right-hand side respectively.

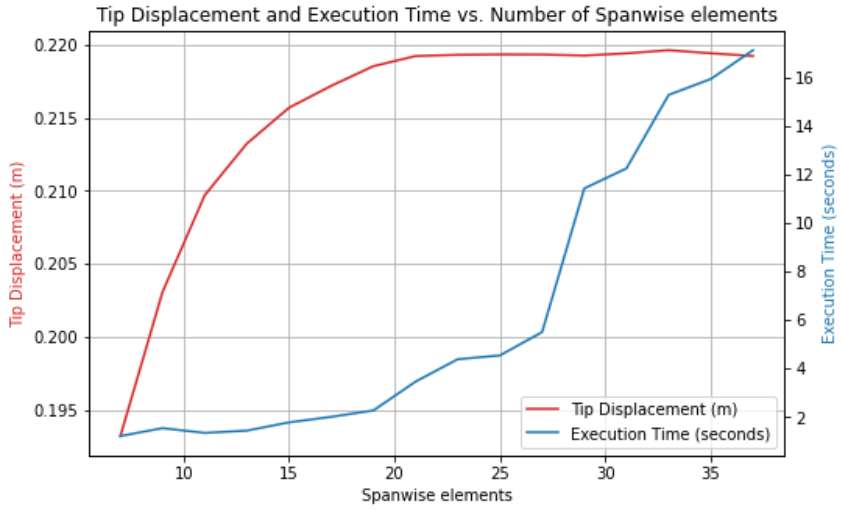

Figure 3: Variation of the vertical displacement of the wing tip and execution time with the number of elements in the spanwise direction.

As can be seen in the aforementioned figures as the number of elements of the mesh increases, the coefficients of lift and drag, the tip displacement and fuel burn will converge. It can also be seen that

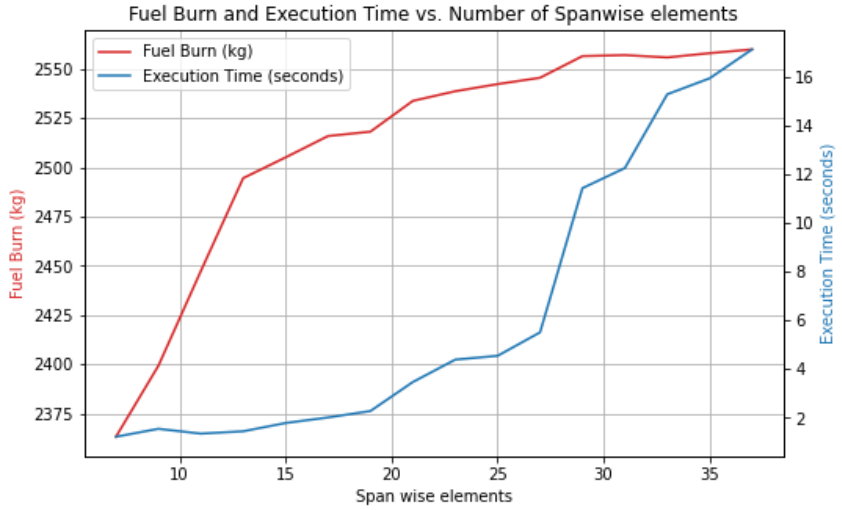

Figure 4: Variation of the fuel burned and execution time with the number of elements in the spanwise direction.

the computational cost, here represented by the execution time, grows exponentially and it´s value is expected to be even greater during an optimization. A equilibrium must therefore be found between grid independence and computacional cost.

A mesh with 5 elements in the chordwise direction and 19 elements in the spanwise direction was chosen. For this mesh the values of lift and drag coefficients for both surfaces and vertical wing tip displacement have already converged and the difference to the fuel burn converged value is around 1.5%. This mesh provids therefore accurate results while keeping the computational cost relatively low.

2.4 Control points study

In order to ensure that the results obtained from the optimization were sufficiently accurate and independent from the amount of control points used for each variable, the full optimization problem was solved using different amounts of control points for the wing twist, chord, spar thickness, skin thickness and thickness over chord.

One should note that with this approach while varying the amounts of points of one of the variables in study, the amount of points of the others was fixed to four. This fixed amount of points in the other variables will influence the results, and therefore these results must only be taken as indicative for determining a suitable value for the amount of control points.

As can be seen from Table 3, using 3 control points for the Twist, Chord, Thickness over Chord, Spar thickness and Skin Thickness is reasonable taking into account the wing size and the small variations in the lift and drag coefficients and wing tip displacement obtained.

In the horizontal stabilizer case a control point study was not necessary due to the tail size. It was determined that the Twist, Thickness over Chord, Spar thickness and Skin Thickness would have one control point while the chord would have two control points.

Table 3: Variation of the number of control points of Twist, Chord and Thickness to Chord ratio and its effects on the values of Lift and Drag coefficient, represented by the absolute difference between the current value and the previous one. Variation on the number of control points for the Spar Thickness and Skin Thickness and its effects on the value of the vertical wing tip displacement.

	Aerodynamics						**Structures**	
Points	**Twist**		**Chord**		**Thickness/chord**		**Spar thickness**	**Skin thickness**
	Diff CD	**Diff CL**	**Diff CD**	**Diff CL**	**Diff CD**	**Diff CL**	**Diff Disp [m]**	**Diff Disp [m]**
1	—-	—-	—-	—-	—-	—-	—-	—-
2	0,00145	0,0189	-0,0006	-0,0158	0,0004	-0,00299	0,016419154	-0,000773762
3	-0,0019	-0,023	0,00169	0,00563	-0,0006	-0,01507	-0,015852951	0,000357192
4	-0,0002	-0,011	-0,0017	-0,0084	-0,0002	0,000227	-0,000229784	-1,82478E-05
5	2,5E-05	0,005	0,0011	0,0124	0,0042	0,014494	0,000133655	0,000206069
6	5,5E-05	-0,004	-0,0007	-0,0018	0,14154	-0,00797	0,000312885	-0,00026338

2.5 N^2 and Disciplines Coupling

In this work, the aim is to perform an aerostructural optimization of two wings. Thus, the aerodynamic and structural components will be directly linked and will mutually affect each other. The most evident interactions in the aerostructural analysis will arise from the fluid-surface interaction, where aerodynamic forces will be applied, thereby influencing the structural part to some extent. On the other hand, the wing's structure will influence the aerodynamic performance, particularly through changes in shape and mass of the wings during the optimization process.

The diagram in Figure 5 illustrates the coupling of the aerodynamics and structural analysis disciplines. These two disciplines will provide data for calculating the aircraft's performance and are based, respectively, on the Vortex-Lattice Method (VLM) and the finite element analysis of the wingbox.

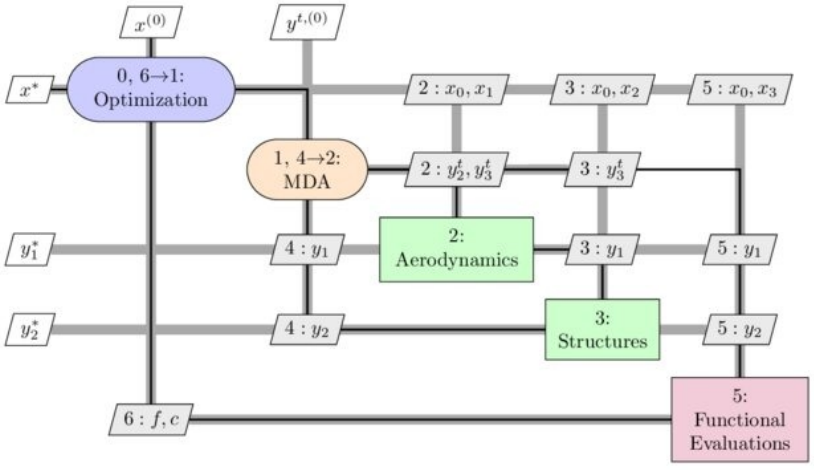

Figure 5: XDSM diagram of the aerostructural problem

The N2 diagram, Figure 6, represents the interactions between the aircraft surfaces (wing and tail) and the aerostructural points (AS point 0 and AS point 1) in a specific case study. Each aerostructural point has both aerodynamic and structural functions, which include failure criteria to ensure the integrity of the surfaces during flight. Additionally, there are performance groups assigned to each surface and the entire aircraft. These functions and groups are interconnected through coupling relationships. The main

objective is to optimize this model considering the different disciplines involved and their interactions.

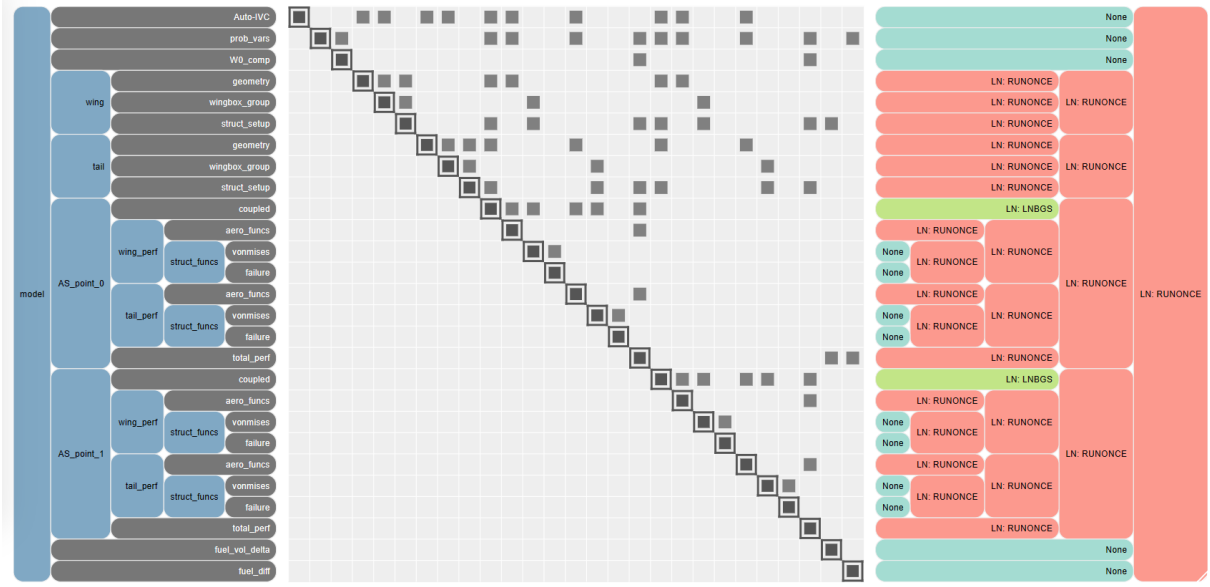

Figure 6: N^2 diagram of the full optimization problem.

3 Aerostructural Optimization

By running an analysis of the defined baseline of the aircraft it is possible to verify that the fuel burn is 2434.27 kg, the wingbox mass is 2346.15 kg and total aircraft mass is 37986.02 kg. The wing cruise CD and CL are 0.02643854 and 0.56280648 and the tail cruise CD and CL are 0.01836319 and -0.05215069, respectively.

Having defined the model, through the definition of the objective function, the design variables, the constrains, the baseline, the mesh and the amount of control points, the aerostructural optimization is ready to be performed.

The optimizer chosen for this task was the SLSQP. The number of maximum iterations allowed was the default of 200 but the tolerance for termination was set to 1×10^{-4} instead of the default 1×10^{-6}, which will still allow for accurate results but reduced computational time.

Throughout the project multiple optimizations were performed, some more successful than others. These optimizations were carried out varying the combination of design variables, the amount of constrains and the bounds considered. Many of the optimizations performed were discarded as they either failed or presented unrealistic results which made no physical sense. From this failed attempts lessons were learned, and more realistic boundaries and appropriate mesh sizes were adopted. From all the successful attempts two were chosen to be presented in this report.

3.1 First Optimization

The first optimization chosen to be presented in this study has as its objective function the fuel burned during cruise.

Table 4: Summary of the constrains applied in the first optimization.

Constrain	Initial value	Lower Bound	Upper Bound	Optimum
L equals W in cruise	0.047	-0.001	0.001	0.00099
L equals W in maneuver	0.610	-0.001	0.001	0.00099
Fuel Consistency	2.971	0	0	-6.9e-09
Fuel to Wingbox volume	2.873	0	-	2.588
CM in cruise	0.014	-0.001	0.001	0.001
CM in maneuver	0.0139	-0.001	0.001	-0.00099
Wing failure in cruise	-0.660	-	0	-0.5159
Wing failure in manouver	-0.722	-	0	1.07e-05
Tail failure in cruise	-0.831	-	0	-0.9495
Tail failure in manouver	-0.826	-	0	-0.905

For design variables the cruise angle of attack, α, and the maneuver angle of attack, $\alpha_{maneuver}$, were considered. In addition to those the wing´s twist control points and sweep were also chosen to be design variables in order to influence the aircraft´s aerodynamics, especially the lift and drag coefficients. In order to influence the structural side of the aircraft the parameters spar and skin thickness for both the wing and horizontal stabilizer were chosen as design variables. The fuel mass was also added as a design varible.

All these design variables were chosen for the optimization having in mind the constrains which were to be imposed.

In order to guarantee the trimming of the aircraft it was imposed that, for both flight conditions, the lift produced should equal the weight of the aircraft and that the aircraft´s pitching moment was zero. In terms of structural constrains it was imposed that, for both flight conditions, the wing and tail should not structurally fail, meaning having stress values below the Von Mises failure limit. It was also imposed that at the root of the wing the twist should be zero. Constrains were also added to ensures that the wingbox had enough internal volume for the fuel and that fuel mass value is the same as the fuel burn mass computed from the cruise point for consistency purposes. The constrains and their respective bounds are summarized in Table 4. The pitching moment and lift equal to weight constrains were loosen up, by using a bound very close to zero instead of an equality, to facilitate the optimization while maintaining the required accuracy.

After setting these design variables and constrains the optimization was ran successfully (exit mode 0). The optimization required 14 iterations, 18 function evaluations and 14 gradient evaluations.

It was determined that the fuel burned was 2845.879 Kg and the wingbox mass was 2903.15 Kg which is higher than the baseline. The total mass of the aircraft at takeoff was 34971.97 Kg, which is in line for what is expected for a commercial regional jet like the one studied. The center of gravity of the airplane was located along the longitudinal axis, 1.876 meters forward from leading edge of the wing. The aircraft vertical wing tip displacement was 0.4258 meters which reveals a level of aeroelasticity that is expected from such aircraft. In cruise, the wing lift and drag coefficients were 0.4453734 and 0.02152682 and the tail´s were 0.20204918 and 0.02939031, respectively. These values of CL and CD are reasonable for the size of the lifting surfaces.

In Table 5 the initial values defined as the baseline, the upper and lower bounds and the optimum

Table 5: Initial baseline values, upper and lower bounds and optimum solutions for the design variables.

Design Variable	Initial Value	Lower Bound	Upper Bound	Optimum
Alpha [°]	0	0	5	1.5193
Alpha Maneuver [°]	0	-15	15	9.189
Wing Twist [°]	[4,6,8]	0	8	[8, 7.25, 4.06e-13]
Wing Sweep [°]	30	0	60	0
Wing spar thickness [m]	[0.004, 0.005, 0.008]	0.003	0.1	[0.0138, 0.0997, 0.0999]
Wing skin thickness [m]	[0.005, 0.01, 0.015]	0.003	0.1	[0.003, 0.0072, 0.0039]
Tail spar thickness [m]	[0.002]	0.001	0.03	[0.03]
Tail skin thickness [m]	[0.001]	0.001	0.03	[0.022]
Fuel Mass [Kg]	10000.0	0	200000	2845.879

solution for the design variables can be seen. In Figure 7 the optimized wing and horizontal stabilizer lift distribution, twist, thickness to chord ratio, spar and skin thickness and failure criteria can be observed as well as a graphical representation of the wing and tail meshes deformation and engine location.

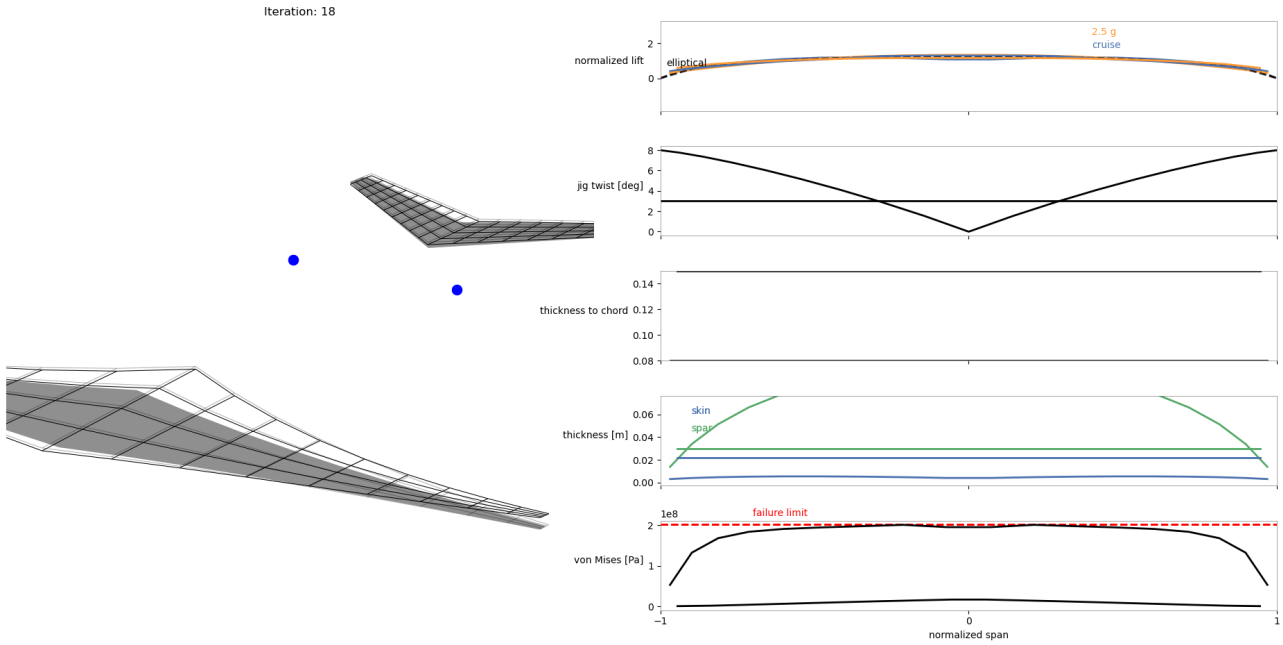

Figure 7: Optimized wing and horizontal stabilizer lift distribution, twist, thickness to chord ratio, spar and skin thickness and failure criteria. Graphical representation of the wing and tail meshes deformation and engine location.

As it can be seen from the optimal solutions of the design variables the values for the angles of attack in cruise and maneuver are within what is expected. The wing twist distribution is also according to reasonable limits and its value at the root is zero as it was constrained. It should be noted that usually the twist is negative, known as washout, but in the particular case studied, from previous iterations of optimizations, better results were obtained using a positive twist, know as washin, and therefore the twist was bounded to positive values. In the optimal configuration found, the wing did not present any sweep as opposed to the initial baseline.

The thickness of the wing spar demonstrated a gradual reduction towards the wingtip, as anticipated. However, the measured thickness of 99 mm exceeds the typical range observed in commercial aircraft, where spar thicknesses generally fall between 5 mm and 25 mm [7]. The upper bound limitation in this

case is excessive and will need to be reduced in future optimizations.

The tail spar thickness has a value of 30 mm, which is the upper bound, and as in the wing spar case this value is a little excessive.

The values determined for the wing skin thickness are within what is used in the industry, where values range from 1 mm to 7 mm [8]. The tail skin thickness has a value much superior than what would be expected and so the upper bound should be lowered in future optimizations to prevent this.

From Figure 7 it can be seen that the tail twist has a constant value of 3, the baseline value, across the entire span, while the wing twist distribution increases from zero at the root to 8 at the tip. The lift distribution, in both cruise and maneuver, is very close to the ideal elliptical lift distribution which minimizes induced drag. It can also be observed that both the wing and the horizontal stabilizer are below the failure criteria but that near the root the structure is very close to this limit.

In Figure 8, the optimization history of some of the design variables, constrains and objective functions is shown.

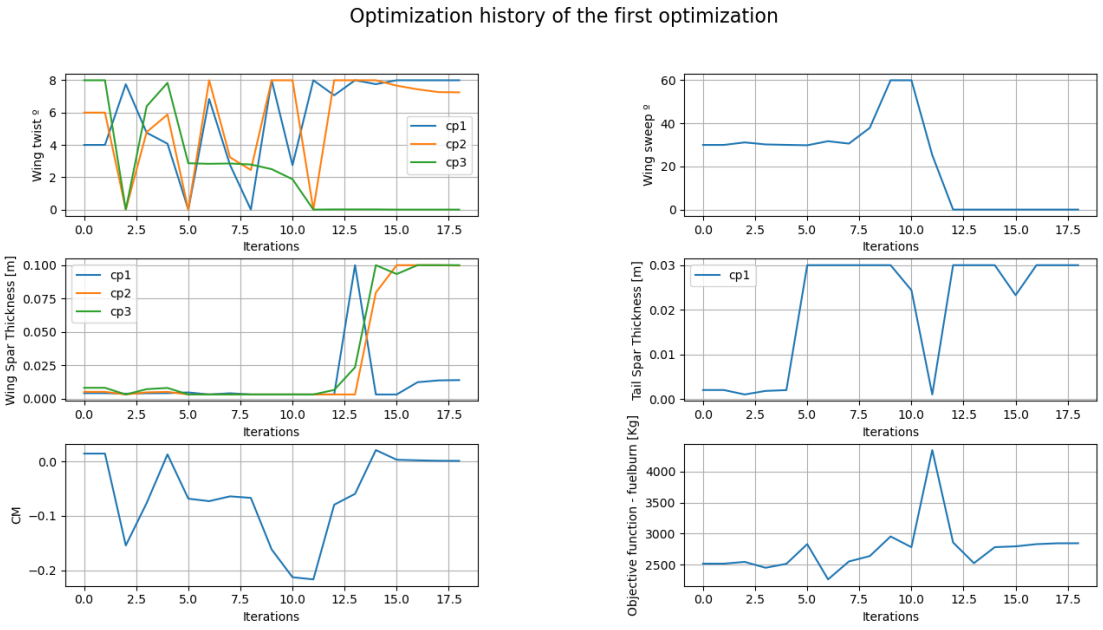

Figure 8: Variation of the value of the wing twist control points, the wing sweep, the wing and tail spar thickness control points, the pitching moment and the fuel burn with the number of iterations.

In general, it can be seen that around the 13th iteration mark, changes in the value of the design variables, constrains and objective function occur. After this mark the values stabilized around their final optimal value.

The wing sweep starts at 30 degrees, the baseline, until around the 8 iteration when it jumps to the upper bound of 60 degrees. After the 10th iteration this value goes to 0 where it remains until the end of the optimization. It can also be seen that the control points for the wing and tail spar thickness increase significantly their values around the 13 iteration. It is just before this mark that the objective function, fuel burn decreases its value, which had been growing throughout the iterations, to a value close to the optimal.

Overall, this first optimization provided good results with the exception of the large spar and skin thickness. More attention should be paid to the values of the upper bounds of these design variables in future optimizations.

3.2 Second Optimization

Building on the previous results a new optimization was set up. In this new optimization, three design variables were added: the wing´s thickness over chord control points, the tail twist and the tail span. These new design variables will allow for a greater design space when it comes to aerodynamic optimization.

In addition to this new design variables a new aerodynamic constrain was also added. With this constrain the profile coefficient of lift will be limited to 0.6 during cruise to avoid stall.

In this new optimization many of the previous constrains and design variables had their bounds changed and corrected. This new bounds can be seen in Table 6, which contains the summary of the new constrains, and in Table 7 which contains the design variables initial values, new bounds and optimal solutions after optimization.

This new optimization, with the added constrain and design variables ran successfully (exit mode 0). The optimization required only 6 iterations and gradient evaluations and 7 function evaluations.

The fuel burned was determined to be 2218.8 Kg, which is 625 kg less than in the previous optimization, and the wingbox mass was 1386.46 Kg which is less than half than in the first optimization. The total aircraft mass was also reduced to 29040 Kg. The wing´s lift and drag coefficient remained approximately the same at around 0.43494374 and 0.02119818, respectively. The horizontal stabilizer drag coefficient had a slight decrease to 0.02195308 but the lift coefficient decreased by one order of magnitude to 0.02025958. This significant decrease may be explained by changes to the tail twist and span, as it will be seen later on, and due to the fact that less lift is needed from the horizontal stabilizer in order to trim the aircraft. The reduced need of trimming from the horizontal stabilizer can be explained by the shift in the center of gravity which now is 70 cm forward from the leading edge of the wing along the longitudinal axis.

As can be seen from Figure 7 there was an increase of 3 $^\circ$ in the angle of attack in cruise and maneuver, which are now 4.85 $^\circ$ and 12.123 $^\circ$, respectively. This new values are still within the typical range of what would be expected, although a bit higher than the norm. In this new optimization the wing presents almost no twist across its span and a sweep angle of 17.16 $^\circ$, unlike in the previous optimization where there was twist but no sweep.

The twist of the horizontal stabilizer is -2.097 $^\circ$ and its span is 4.575 meters. The fact that the twist is now negative and the span decreased by about 5 meters justifies the great reduction in the coefficient of lift.

The thickness to chord ratio increased at the middle of the wing from 8% to 10 % but remained the same at the tip and root.

As stated in the previous section, the values for the spar and skin thickness considered in the previous

Table 6: Summary of the constrains applied in the second optimization.

Constrain	Initial value	Lower Bound	Upper Bound	Optimum
L equals W in cruise	0.0514	-0.001	0.001	-0.00099
L equals W in maneuver	0.6097	-0.001	0.001	0.00048
Fuel Consistency	3.108	0	0	-2.62 e-06
Fuel to Wingbox volume	2.322	0	-	3.020
CM in cruise	-0.0046	-0.01	0.01	0.0243
CM in maneuver	-0.005	-0.01	0.01	-0.069
Wing failure in cruise	-0.6651	-	0	-0.587
Wing failure in manouver	-0.725	-	0	1.531e-05
Tail failure in cruise	-0.873	-	0	-0.9633
Tail failure in manouver	-0.864	-	0	-0.9475
Cl_max in cruise	[0.547, 0.609, 0.629, 0.635, 0.628, 0.609, 0.579, 0.537, 0.482]	-	0.6	[0.565, 0.599, 0.586, 0.558, 0.523, 0.482, 0.438, 0.390, 0.340]

Table 7: Initial baseline values, upper and lower bounds and optimum solutions for the design variables of the second optimization.

Design Variable	Initial Value	Lower Bound	Upper Bound	Optimum
Alpha [°]	0	0	5	4.853
Alpha Maneuver [°]	0	-15	15	12.126
Wing Twist [°]	[4,6,8]	0	15	[9.3e-2, 7.4e-1, 2.4e-17]
Wing Sweep [°]	30	0	60	17.16
Wing spar thickness [mm]	[4, 5, 8]	5	30	[5.05, 5.05, 5.07]
Wing skin thickness [mm]	[5, 10, 15]	3	10	[4.53, 6.64, 7.76]
Wing t/c	[0.08, 0.08, 0.08]	0.07	0.2	[0.08, 0.10, 0.08]
Tail Twist [°]	3	-5	15	-2.097
Tail span [mm]	[9,3749]	1	11	[4.575]
Tail spar thickness [mm]	[2]	5	30	[29.79]
Tail skin thickness [mm]	[1]	2	10	[10]
Fuel Mass [Kg]	10000.0	0	200000	2218.8

optimization were to large, and so the upper bounds were reduced to 30 mm and 10 mm, respectively. This changes had the desired effects on the results. The wing spar thickness is now 5 mm, a very reasonable value, which remains almost constant throughout the span of the wing and the wing skin thickness decreases from 7.76 mm at the root to 4.53 mm at the tip, being consistent with the usual values for commercial aircraft. In the horizontal stabilizer, these values are a bit larger, being the spar and skin thickness 29.79 and 10 mm, respectively. Although very close to the upper bounds defined, the values are still within an acceptable range from reality.

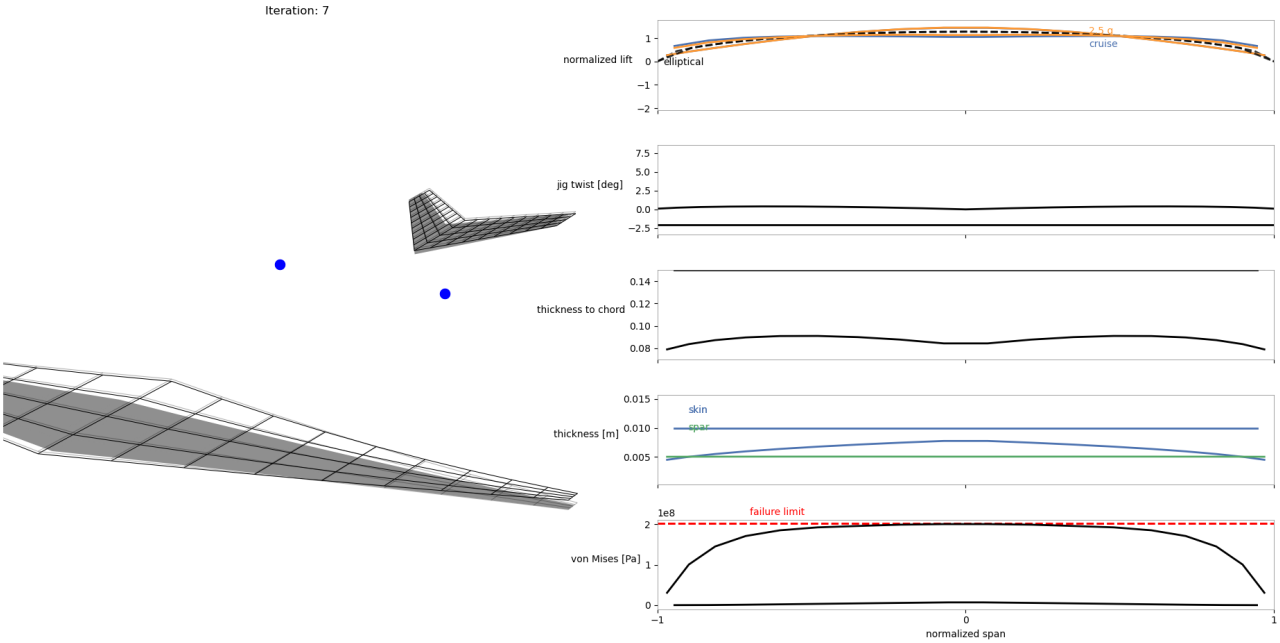

Figure 9: Optimized wing and horizontal stabilizer lift distribution, twist, thickness to chord ratio, spar and skin thickness and failure criteria. Graphical representation of the wing and tail meshes deformation and engine location.

From Figure 9 it can be seen that the wing and tail lift distribution, for both cruise and during maneuver, is not quite an elliptical distribution, although it is very close. This discrepancy is especially true during the maneuver. It can also be seen that the wing presents almost no twist and that the horizontal stabilizer has a negative constant twist. The thickness to chord ratio of the profile increases from the root up until the middle of the wing, from 8% to 10% and then proceeded to decrease back to 8% at the tip. The stress values applied to the lifting surfaces are below the Von Mises failure limit and so the structures will not fail. Closer to the root of the lifting surfaces the value of the stresses are higher. On the left hand side of Figure 9 it can be seen that the mesh is much more dense near the wing tips, for reasons already mentioned. It can also be seen the vertical wing tip displacement of 0.3593 meters.

It can be seen from the optimization history of Figures 10 and 11 that the most relevant changes occur in the first 3 iterations of the optimization and that afterwards the values slowly converge to their optimal solution.

On the tail the twist tends immediately to a negative value and the span to be smaller, unlike the spar thickness which tends to the upper limit. The opposite occurs on the wing spar thickness which tends to the lower bound in all control points. At the wing the twist tends to zero and the sweep decreases rapidly

to 17 degrees.

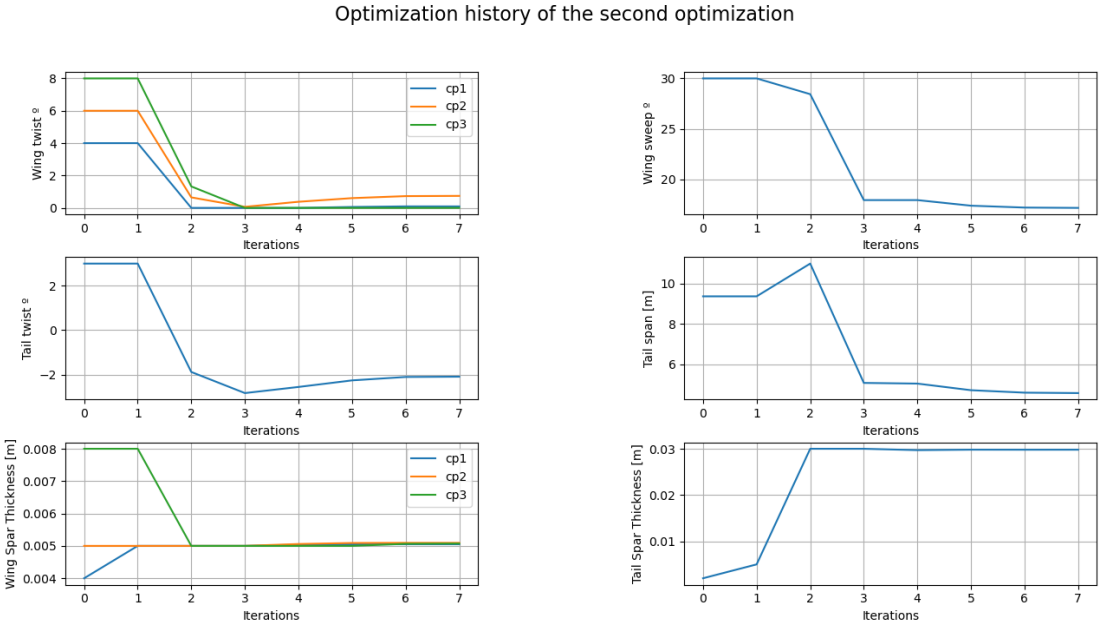

Figure 10: Variation of the design variables values of wing and tail twist, the wing sweep, wing and tail spar thickness and tail span with the number of iterations.

From the optimization history of Figure 11 it can be seen that initially only the four control points closest to the root of the wing verified the lift coefficient constrain during cruise. At the end of the optimization the lift coefficient distribution is Cl= [0.566 0.599 0.586 0.5580.523 0.482 0.438 0.390 0.340], and so it can be said that the constrain is verified and that in general the section lift coefficient increases from root to tip.

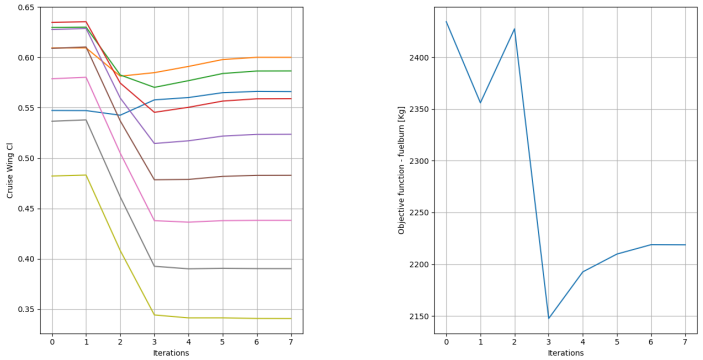

Figure 11: Variation of the lift coefficient constrain during cruise and the fuel burn with the number of iterations.

3.3 Lift coefficient constrain during manoeuvre

The attempts to add the lift coefficient constrain to the maneuver flight point, and therefore use all constrains which were proposed at the beginning of this report, were unsuccessful.

Using only the design variables present in the last optimization no solution was found and so the wing´s chord was added as new a design variable. This was done in the hope of achieving a new chord distribution that would allow a decrease in the section lift coefficient.

The multiple attempts which were made with all design variables were discarded, even though they were successful in the sense that OpenMDAO reached a solution (Exit mode 0), as the values reached had no relevant physical meaning. For instance, in many of the optimizations, the values of the chord at the tip were too large to be feasible in an regional airplane as the one being studied. In many instances these values reached 6 meters and when constrains were added to ensure this would not occur the optimization proceeded to fail.

This problem might be overcame by using a more refined mesh at the tip of the wings and loosening up some of the bounds of the constrains.

3.4 Model short falls

OpenMDAO seeks to mimic what happens in reality in order to explore the design space and provide the best optimum solution based on the constrains proposed, the design variables and the objective function.

The current aerostructural optimization problem involves a large number of design variables which leads to high-dimensional design spaces. As exploring such spaces can be computationally expensive, a sparser mesh was used than what would be ideal. Despite this fact acceptable engineering solutions for a preliminary design were obtained.

Achieving tight coupling between the aerodynamic and structural solvers is crucial for accurate results in aerostructural optimization. However, achieving this coupling can be challenging, particularly when dealing with nonlinearities or dynamic problems as is the case.

OpenMDAO uses a low-fidelity aerodynamic model based on the Vortex-Lattice Method (VLM) using a formulation with horse-shoe vortices to perform its aerodynamics analysis. The VLM models the lifting surfaces of an aircraft as an infinitely thin sheet of discrete vortices to compute lift and induced drag. Some of the assumptions that the VLM considers is that the flow field is incompressible, inviscid and irrotational and that the angle of attack and the angle of sideslip are both small.

These assumptions are not always verified in the case that is being studied, for instance from the optimization it can be seen that the angle of attack is not small.

Even though the VLM studies incompressible and inviscid flows, OpenMDAO allows for the influence of viscosity to be added to the analysis as well as the the wave drag which is typically not directly considered in the VLM method. Both this options were activated during the optimizations performed. As stated before OpenMDAO accounts for the drag from the fuselage, tail surfaces, nacelles, and pylons even though they are not being modeled.

Despite all of this, the model does not take into account the flow separation and the interference of the flow from one lifting surface to another. Also the VLM method is based on the thin airfoil theory, which may not be suitable for the particular case being studied, taking into account the thickness to chord ratio

and the chord size of the wing. The implementation of the panel method should be considered as an alternative.

OpenMDAO uses a low-fidelity structural model based on a wingbox using a formulation with 6 degrees of freedom 3-D spatial beams to perform its structural analysis. This model allows for the estimate of the weight of other components not modeled in the wingbox structure (e.g., overlaps, fasteners, etc.) as well as the distribution of the loads from the fuel and the weight of the wingbox across its span.

In the model the stress constraints for the FEM elements were aggregated into a single constraint using the Kreisselmeier–Steinhauser function in order to reduce computational cost during optimization by replacing a large number of constraints with a single constraint.

Some of the short falls of the structural model are that it assumes that the material is isotropic and the fact it can´t capture dynamic effects, such as vibrations.

The model also assumes linear elastic behavior, neglecting nonlinear effects such as material nonlinearity, geometric nonlinearity (large displacements or rotations), or contact interactions. The model cannot therefore accurately represent the actual behavior of the wingbox under extreme loading conditions as is the case during the maneuver.

The current model being used also uses a simplified geometry, considering only two spars and it does not provide the ability to vary the number of ribs of the wingbox. Buckling cannot be modeled and there is no buckling constraints.

The model cannot capture local effects, such as stress concentrations around fastener holes, and so it provides averaged or global responses which are not suitable for detailed stress analysis at the local level.

4 Conclusions

In summary, this project has demonstrated that optimization is a multifaceted process that requires careful consideration and evaluation. When employing an optimizer with a set of design variables, constraints, and an objective function, it is crucial for engineers to critically assess the feasibility and realism of the solutions generated, while establishing appropriate bounds and constraints that reflect real-world scenarios.

The significance of convergence criteria and mesh refinement has been evident throughout this project. Utilizing refined meshes and stringent convergence criteria, while optimizing computational resources, is essential to avoid results that deviate from real-world behavior and to prevent premature solutions and local minima.

The selection of the design variables significantly influence the solution design space and the identified optima. It is also important to choose baseline values for design variables that are close to the optimal solution, as distant baseline values can lead to the risk of suboptimal solutions being identified by the optimizer in search of the overall best solution. For instance in this particular project, errors were made in the initial selection of wing twist values as they were to far away from what was being imposed by the constrains.

Overall, the final optimization has been successful in achieving significant reductions in fuel consumption (over 200 kg) as well as in the overall weight of the wingbox and aircraft. These preliminary outcomes can be further enhanced by implementing the suggestions provided throughout the report and conducting additional optimization iterations. The preliminary analysis conducted in this project should be followed by a more comprehensive study in line with what the optimization direction indicated to create a new optimized aircraft. This analysis should be done using high fidelity models.

References

[1] Skybrary. Bombardier regional jet crj-700. https://www.skybrary.aero/aircraft/crj7.

[2] A. Tools. Nasa sc(2)-0612 airfoil (sc20612-il). http://airfoiltools.com/airfoil/details?airfoil=sc20612-il, .

[3] A. Tools. Naca 0015 (naca0015-il). http://airfoiltools.com/airfoil/details?airfoil=naca0015-il, .

[4] A.-A. specification metals. Asm-aluminum 7075-t6; 7075-t651. https://asm.matweb.com/search/SpecificMaterial.asp?bassnum=ma7075t, .

[5] A.-A. specification metals. Asm-aluminum 7075-t6; 7075-t651. https://asm.matweb.com/search/SpecificMaterial.asp?bassnum=ma7075t, .

[6] ExxonMobil. Exxonmobil jet fuel. https://www.exxonmobil.com/en-bd/commercial-fuel/pds/gl-xx-jetfuel-series.

[7] S. Francis. A350 a400m wing spars: A study in contrasts. https://www.compositesworld.com/articles/a350-a400m-wing-spars-a-study-in-contrasts, 1 2013.

[8] B. K. Stanford and P. D. Dunning. Optimal topology of aircraft rib and spar structures under aeroelastic loads.